

Optimal Electrification of Off-grid Smart Homes Considering Flexible Demand and Vehicle-to-Home Capabilities

Marcos Tostado-Véliz, Rogelio S. León-Japa Francisco Jurado*

Department of Electrical Engineering, University of Jaén, 23700 EPS Linares, Jaén, Spain

*Abstract - The emergence of novel demand-side management strategies is provoking that residential consumers cannot be longer categorized as inflexible loads. In that sense, new paradigms such as flexible demand and vehicle-to-home capabilities have appeared on pursuing a more efficient management of the different domestic assets such as smart appliances, small renewable generators and storage facilities. Consideration of such kind of management strategies plays a vital role on designing stages of electrifications systems for isolated homes. In this regard, a proper evaluation of possible demand-side capabilities enables a more accurate evaluation of the electrification project. This paper tackles this issue by developing a **Mixed Integer Linear Programming** formulation for optimal planning of electrification systems for off-grid dwellings. The developed framework allows to incorporate and analyse advanced demand-side strategies such as deferrable loads and vehicle-to-home processes by evaluating different project costs over various time horizons. The proposed approach is applied to a benchmark off-grid residential case study and various results are provided and analysed. As the most relevant result, **it** is worth remarking that total project cost can be reduced by ~21.2% and ~25.73% by considering flexible demand and vehicle-to-home capabilities, respectively. Nevertheless, the highest monetary savings were achieved when both strategies are jointly adopted, reducing the total project cost up to ~41.5%. The reported results demonstrate the importance of considering the different demand-side strategies on planning stages of electrification systems for off-grid dwellings.*

Keywords: Off-grid smart home, Flexible demand, Vehicle-to-home, Mixed-Integer

Linear Programming

*Corresponding author, Tel.: +34 953 648518; Fax: +34 953 648586.

E-mail addresses: fjurado@ujaen.es (F. Jurado), mtostado@ujaen.es (M. Tostado-Véliz), rleonj@outlook.es (R. S. León-Japa)

Nomenclature

Acronyms

BES	Battery Energy Storage
DEG	Diesel Engine Generator
EWH	Electric Water Heater
HEM	Home Energy Management
HOMER	Hybrid Optimization Model for Electric Renewable Energies
HVAC	Heating-Ventilation-Air conditioning
MILP	Mixed Integer Linear Programming
PV	Photovoltaic
PEV	Plug-in Electric Vehicle
SOC	State-of-Charge
V2H	Vehicle-to-Home

Set (Indexes)

$\mathcal{Y}(y)$	Year
$\mathcal{R}(r)$	Representative day
$\mathcal{T}(t)$	Hour
$\mathcal{K}(k)$	Deferrable appliance
\mathcal{E}	Cluster of a representative day

Superscripts

DEG	Diesel Engine Generator
PV	Photovoltaic system
Inv	Inverter
BES, ch/dch	Battery energy storage in charging/discharging mode
PEV, ch/dch	Electric vehicle in charging/discharging mode

App, d/nd	Deferrable/non-deferrable appliance
HVAC, h/c	Heating-ventilation-air conditioning system in heating/cooling mode
air, in/out	Indoor/outdoor air
EWH	Electric water heater
w, h/c	Hot/cold water
sp/db	Set-point/dead-band
build	Building
$\overline{(\cdot)}/\underline{(\cdot)}$	Maximum/minimum value of a variable or parameter
$\widehat{(\cdot)}/\overline{(\cdot)}$	Arrival/departure
<i>Parameters</i>	
$\Delta\tau$	Time step (h)
r	Inflation rate (-)
κ	Capital costs
ν	Replacement costs
μ	Operation and maintenance costs
γ	If equals to 1, indicate that an element has to be replaced (Binary)
σ	Function that represents variation of fuel consumption through project lifetime
α, β	Fuel consumption coefficients (litre/kW)
λ	Fuel cost (\$/litre)
ρ	Carbon tax (\$/ton)
φ	CO ₂ emissions factor (kg/litre)
T	Expected lifetime of assets (h)
ω_r	Number of days through a year that can be characterized by the representative day r

η	Efficiency (-)
DOD	Depth of discharge (pu)
Ω	Time window ($\Omega_k = [LB_k, \dots, UB_k]$)
ϑ	Solar irradiation (kW/m ²)
θ	Temperature (°C)
δ	Time slots of the duty cycle of a deferrable appliance
M	Mass (kg)
R	Equivalent thermal resistance
C	Thermal capacity
v	Volume (gal)
COP	Coefficient of performance (pu)
Ψ	Maximum allowed sizing of assets
Y	Budget limit (\$)
<i>Decision variables</i>	
p	Power (kW)
ε	Energy (kWh)
on/off	If equals to 1, indicate that a deferrable appliance is activated/deactivated (Binary)
u	Commitment status of assets (Binary)

1. Introduction

According to the last report of the International Energy Agency, around 725 million people do not have access to electricity supply through the world [1]. Typically, this situation corresponds with remote or rural areas, where extending the main electrical grid entails enormous economic costs and technical difficulties [2]. Electrical supplying of

such users is only feasible by deploying onsite generators and storage facilities. Environmental concerns are moving towards wide use renewable-based generators in combination with storage facilities for electrical supplying of isolated dwellings [3]. However, fossil fuels are still widely employed as backup generation to manage with unpredictable and intermittent behaviour of renewable sources [4].

Viability of electrification projects for off-grid houses is strongly determined by its economic impact on home users, which is in turn influenced by multiple factors like generation and storage technologies, demand or weather parameters. On the other hand, planning tools typically require to handle with a large amount of data [5]. In this regard, designing electrical supplying systems for off-grid homes is not a trivial task. In the literature, this issue is typically tackled by posing optimization frameworks, which are based on different principles and assumptions. Some distinctive related works are reviewed below.

The authors of [6] developed a dynamic simulation approach for sizing a hybrid system for electrical supplying of stand-alone residential loads, which incorporates a proton-exchange-membrane fuel cell as backup generator. By means of the developed tool, different parameters of the fuel cell such as its rated power or time constant are optimized by means of a simulation-based technique. The authors remarked that backup generation size can be notably reduced if its dynamic characteristics are taken into account. A simplified model for optimal planning a **PV-BES** system for an isolated dwelling was developed in [7]. This approach determines the PV array peak power and BES capacity from a deterministic point of view. To that end, mathematical expressions are developed for calculating the different decision variables on the basis of desired autonomy, sunlight hours and energy produced by solar panels. The authors demonstrated that energy cost can be reduced up to 25% by using the proposed approach. Chen

developed in [8] an efficient methodology for sizing PV-BES systems for stand-alone homes. This approach is based on directly computing the different design variables without simulating the study system. Prospective weather variations during the project lifetime are also considered. The author claimed that his methodology can obtain accurate results in a much more efficient way compared with other traditional techniques. PV system peak power and storage capacity for electrification of isolated dwellings are jointly optimized in [9] by performing a simulation model. Stochastic behaviour of solar irradiation is explicitly incorporated within the model to consider large generation fluctuations. The authors highlighted the versatility and modularity of their model. Kazem, et al [10], proposed a deterministic optimization framework for isolated PV residential installations, concluding that solar generation can be increased by 20.6% for an off-grid home case study at Sohar, Oman. Ghafoor and Munir [11] compared two options for isolated housing electrification, showing that electrical supplying by means of an autonomous PV-BES system is much more economically attractive than expanding the distribution grid. A MILP framework for optimal sizing PV systems in stand-alone residential applications was developed in [12]. Relevant aspects such as inverter costs are considered in the proposed optimization process. The developed method is validated through an off-grid case study in Bursari, Nigeria; pointing out that PV-based electrification is about 30% cheaper than the current system based on diesel engine generators (DEGs). Wang, et al., used the software HOMER Pro® [13] in various real case studies. These authors analysed various hybrid renewable-based configurations, such as Wind-DEG-BES in [14], PV-Wind-DEG-BES in [15], and PV-Wind-BES in [16] for different residential applications. In these research, the authors further developed model predictive controls in order to simulate the systems under study; however, the procedure used in these references is sequential and did not incorporate the impact of the control

strategy in the planning process. The authors of [17] developed a deterministic optimization framework for off-grid PV-BES systems taking into account reliability against components failure. Optimization of the system is performed from a deterministic point of view; this way, PV panels are sized according to the measured peak power, then, a load management strategy is posed in order to simulate the system and size the BES bank accordingly. Complexity and large amount of data involved on planning processes have recently motivated the usage of metaheuristic techniques to manage with this problem. Such is the case of the Particle Swarm Optimizer, which has been considered for various recent studies. On the one hand, Mokhtara, et al [18], used it for designing a hybrid renewable system for electrical supplying of an isolated residential load. The authors found in this study that Wind-DEG resulted the best configuration for the system under consideration. On the other hand, Yoshida and Farzaneh [19] applied it for optimal designing a PV-Wind-DEG-BES system for a case study in Japan, considering the grid balance as the unique constraint of the problem.

As has been shown, a wide variety of techniques, tools and approaches have been proposed over years for tackling with designing purposes in isolated residential systems. However, the existing methodologies still show some important gaps which has motivated this work and are listed below:

- Most of authors circumvent the complexity of the planning problem by posing deterministic methodologies. Other studies recurred to metaheuristic techniques to solve the developed optimization problem. These approaches present several issues. On the one hand, they only can ensure the reachability of sub-optimal solutions. On the other hand, these kind of formulations are normally case-based developed, i.e. they cannot be easily adapted to different scenarios and casuistry. In contrast, MILP-based formulations are instead recognised as the best option

for solving all kind of optimization problems [20]. This approach is normally capable to find the global optimum, presents a modularity structure and can be solved on common software and tools. One clear exception is the reference [12], however, this reference fails to cover the following points.

- Demand-side management has gained importance nowadays on energy management in dwellings. Indeed, **HEM** systems have emerged as an effective way to significantly reduce energy consumption in smart homes, which is achieved by optimally scheduling the operation of some deferrable and thermostatically controlled appliances [21]. The reviewed solution methodologies normally overlooked the influence of the demand-side management on designing stages of isolated home systems. For instance, in references [14-16] the developed model predictive control is totally ignored at planning stage and applied itself in an isolated manner; while in [18] only flexibility brought by the **HVAC** system is considered in a simple manner, whereas optimal operation of other typical appliances is not fully exploited. Strong evidences show that the adopted demand-side management strategy has a direct impact on planning tasks. This idea is supported by a recent study carried out by the authors [5]. Demand-side management may be even more important in isolated homes and its influence on planning tools should not be ignored.
- The use of electric vehicles is moving forward in order to face environmental concerns [22]. Electric vehicles offer wider capabilities such as the **V2H** technology [23, 24], by which power flow is enabled from/to the vehicle via bidirectional chargers. This way, the on-board storage system can be fully exploited giving great flexibility to the system. This fact has been pointed out recently in [25], where the capability of electric vehicles to offer storage capacity

and even backup generation was **highlighted**. Rightly, it seems clear that the V2H capability of electric vehicles may bring enormous benefits in isolated homes. Despite this evidence, to the best of our knowledge, the V2H concept has not been taken into account by the existing planning approaches for isolated home systems.

This work aims at filling the important gaps numerated above, by developing a novel optimization framework for optimal planning electrical supplying systems for off-grid dwellings. More precisely, the principal contributions of this work are twofold:

- Develop a MILP optimization framework for optimal electrification of off-grid homes. **The main novelty of this work is the proper consideration of flexible demand and V2H capabilities in the planning process. To this end,** the developed formulation fully contemplates flexible demand and V2H capabilities **in an original way, including various cost estimations over different time horizons on the objective function. In this sense, the optimization problem is able to simulate the day-ahead optimal operation of the smart home via a HEM framework [20], in which demand-side strategies are incorporated and their influence in the electrification cost can be estimated.** In this regard, home appliances are classified as customary in other referenced works (e.g. see [20]) into non-deferrable, deferrable and thermostatically controlled, in order to fully exploit the potential flexibility of such kind of loads. On the other hand, a detailed electrical vehicle model is incorporated within the formulation in order to contemplate its V2H capability. In addition, the developed optimization framework allows to extract various results that may be vital to take planning decisions, for example the degree of V2H exploitation, total fuel costs or CO₂ emissions. Thus, the usefulness of the developed tool is for real-life applications is manifested. **To the best of our**

knowledge, this work supposes the first attempt to consider such demand-side strategies in the electrification planning process of off-grid smart homes.

- The developed MILP-based formulation is applied to a benchmark isolated smart home. The main purpose of this point is to provide some insights on the influence that flexible demand and V2H capabilities have on the electrification planning for isolated dwellings. In this sense, extensive results are provided and discussed.

Remainder of this paper is organised as follows. Section 2 overviews the isolated home system under study. Section 3 explains the methodology adopted for optimal electrification of the studied off-grid dwelling. Section 4 presents the developed MILP formulation. Section 5 applies the developed mathematical model to a benchmark off-grid home, and various results are presented and analysed. Finally, the main conclusions are duly drawn in Section 6.

2. Overview of the isolated home system under study

Typically, electrification of isolated houses is achieved by deploying onsite renewable generators. Among the available renewable-based technologies, PV arrays are widely used (without loss of generality, it will be considered onwards that a PV array is the unique renewable-based generator installed); however, other alternatives such as wind turbines may be installed. Choosing between different alternatives is typically based on the on-place availability of natural resources such as solar irradiation or wind speed. In order to manage with the intermittent behaviour of such kind of generation, BES systems are widely employed. These facilities are normally charged during sunlight hours and discharged during night in order to effectively met the home demand. Even so, backup generation is normally required in order to fully satisfy the daily load. Different technologies may be used to that end, however, DEGs are still the most conventional one [19].

Under the umbrella of the smart home concept, HEM systems have emerged as an effective way to coordinate the different assets deployed through home systems [20]. In essence, this kind of programs holistically schedule the operation of the generation and storage facilities and some controllable appliances, on pursuing a cheaper and environmental-friendly operation of the system. Whereby, a HEM system should be capable to, on the basis of some forecasted parameters (typically weather parameters in order to calculate the available renewable generation), perform the most suitable day-ahead scheduling plan for the different residential assets [26].

In this regard, only some domestic appliances can be controlled by the HEM system. Thus, the so-called deferrable appliances can be operated within different time windows over a day time horizon, for convenience. Common examples of deferrable appliances are washing machines and dishwashers [27]. On the other hand, the thermostatically controlled appliances respond to temperature signals and are operated according to them. For example, a HVAC system is devoted on keeping the indoor temperature within comfortable limits; this way, this device should be operated whenever the inside measured temperature requires its action. Other typical thermostatically controlled appliance is the EWH [20], which is devoted on keeping the hot water temperature to be used in multiple housework such as showers. In contrast, the non-deferrable appliances cannot be controlled by the HEM system and they are essentially operated on the basis of home inhabitants' decisions. Typical examples of non-deferrable appliances are fridges, ovens and microwaves. For the sake of summarizing, Fig. 1 pictorially schematizes the home system under study and the energy and communication flows enabled among the different assets.

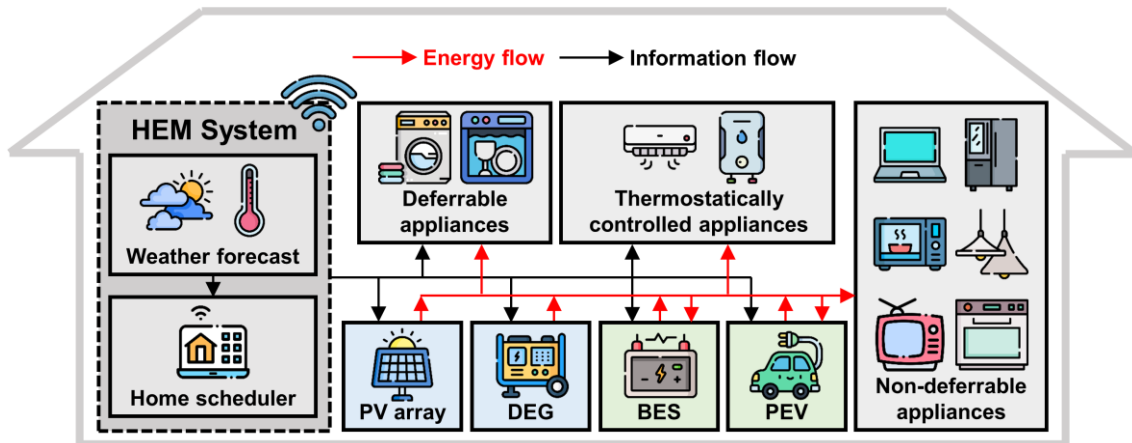


Fig. 1 - Pictorial representation of the isolated home system under study

It is worth mentioning the role of the PEV. During some hours of the day, the electric vehicle is parked at home. At those hours, the vehicle is connected to an onsite installed bidirectional charger which enables both to-home/to-vehicle energy flow (see Fig. 2). This arrangement allows to exploit the V2H capability of the vehicle, so that it can be also seen as a secondary storage facility. Henceforth, it is assumed the HEM system can also schedule the charging-discharging timetable of the on-board PEV batteries. In that sense, it is reasonable that the HEM system requires some information namely, vehicle at-home hours and the expected SOC at arrival time.

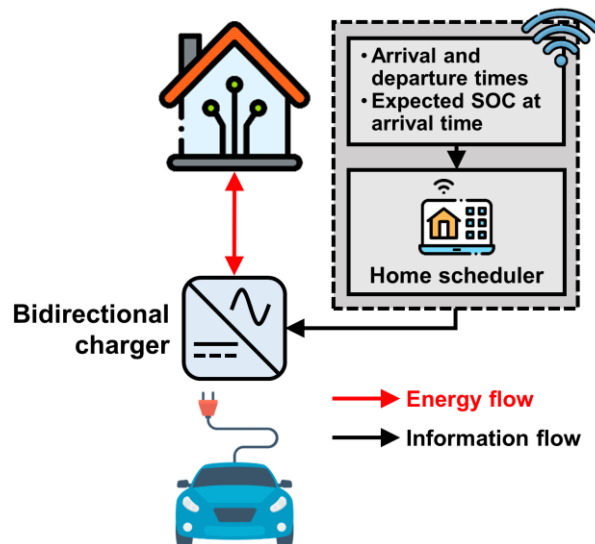


Fig. 2 - Arrangement for electric vehicle charging with V2H capability

To properly coordinate the operation of the different home assets, information flows have to be enabled. The HEM system receives weather forecast signals (temperature and

solar irradiance) and, on the basis of the performed task scheduling, sends control signals to the different controllable devices. That weather information can be easily obtained from public webpages or by using some forecast technique [28]. Due to the considered HEM system is devoted on day-ahead scheduling, two-way communication channels are not, a priori, necessary. In this regard, deviations with respect the scheduling plan are assumed to be addressed by somewhat type of real time control or even through human decisions. Since these tasks are useless in planning concerns, its modelling has not been tackled in this study. Nowadays, smart control of home assets is possible due to the emergence of smart appliances and plugs, which cannot only control the on/off status of a device, but also its power operating point. Thereby, the consumption of some appliances, e.g. HVAC and EWH, can be continuously controlled. Communication flows among the HEM and the PV array, BES and PEV are possible through smart inverters. Such kind of devices allow to control the power injection/absorption of such devices, so that, the charging-discharging plan of storage devices and the generation profile of the PV panels can be scheduled according the day-ahead HEM result. Smart inverters have other interesting capabilities, for instance, they can manage with voltage unbalances, harmonics reduction and reactive power flows [29]. However, such kind of capabilities are frequently online addressed and, consequently, lack of interest in planning stages. Regarding the communication infrastructure, standard and protocols, a rich literature can be found. Since the scope of this paper is very far from further analysing or describing such aspects, the reader is referred to [30, 31] and the references therein for a more detailed information.

3. Developed methodology

This paper develops a methodology for optimal designing electrification systems for isolated homes, which encompasses several stages that are explained throughout this section.

The whole developed procedure is summarized in Fig. 3. As seen, the proposed methodology may be broadly described by three main steps. As customary, electrification planning tools usually start from measured raw data of some necessary parameters. The developed methodology only requires typical weather parameters that are frequently available in public databases (such as ambient temperature and solar irradiation). Other auxiliary information is also required and provided in this stage such as equipment specifications, inflation rate or estimated project lifetime. Secondly, a MILP process is performed in order to determine the optimal components sizing for the home system under study. In this stage, project costs are evaluated over different time scales (see Section 4.1). Some relevant spending has to be evaluated over a daily time horizon. Such is the case of fuel costs of the DEG. In order to properly evaluate this kind of expenditures, the home system is simulated as a HEM problem [20], which can be properly incorporated to the developed MILP-based formulation. Finally, the developed approach is capable to offer a large number of relevant results. Thus, along the components sizing of the designed housing electrification system, this proposal yields, among others, the expected project cost, total CO₂ emissions, the degree of exploitation of V2H capability and fuel consumption.

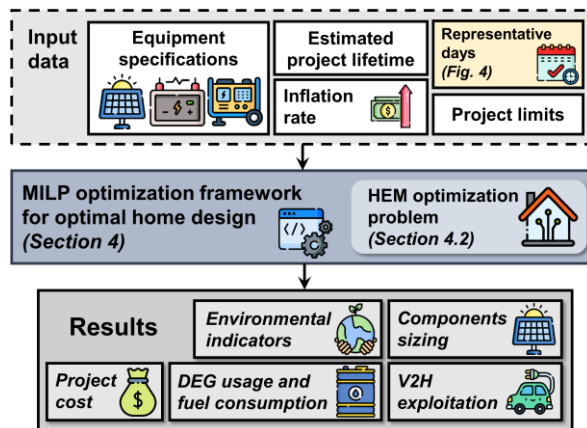


Fig. 3 - Flowchart of the developed methodology

3.1.- Representative Days

In planning stages, large amount of data is usually contemplated in order to achieve reliable and valuable results. Consequently, required information may span for years or even decades [5]. This amount of data may be difficult tractable in practise. On the face of this situation, temporal representation of the available data by means of representative days has been successfully applied in planning stages of multiple electrification systems [32]. In essence, this approach consists on only including in the analysis those profiles that are considered sufficiently representative of the whole data. To that end, clustering techniques are used to group into clusters the most similar daily profiles of the considered parameters. In this paper, the k-medoids technique has been used to this end due to its good features [33]. The k-medoids technique aims at grouping a set of profiles into clusters, within which the members are as similar as possible. This method presents a degree of freedom, namely the total number of clusters. This is a crucial aspect in the clustering procedure as it determines the accurateness of the clustering approximation, however, if the number of clusters is too large, the resulting computational burden may be unaffordable. To help this procedure, the total number of clusters can be set by observing the value of some indicators such as the total sum of distances or the Davies Bouldin index [5]. Once the total number of clusters has been set, the k-medoids method proceeds as the optimal plant location problem (see [33]). Thus, the location of a plant is

interpreted as the representative member of a cluster (called medoid), and the distance of each city with respect the plant is conceived as the dissimilarity of the different clustering members with respect their corresponding medoid. Therefore, the k-medoids is iteratively run to reduce the total sum of distances of the clustering members with respect the medoid. This way, considering the home system described by Fig. 1, historical data respected to solar irradiation and ambient temperature can be characterized through representative profiles (medoids). Thus, the amount of data to be handled can be notably reduced.

As commented, a day-ahead HEM problem is included within the developed MILP planning tool in order to properly evaluate daily fuel consumption of the DEG. Results yielded by the HEM problem are strongly influenced by the SOC of the PEV at its arrival time. This aspect determines the availability of the PEV and, consequently, constraints the time slots in which its V2H capability can be scheduled. This parameter is, a priori, unknown since it depends on the daily mileage [30]. In this work, inspired by [21], the initial SOC of the PEV has been considered a stochastic variable and treated via scenarios. To that end, similar to [21], the initial SOC of the PEV has been modelled as a truncated Gaussian distribution function According to the Law of Large Numbers, stochastic feature of a random variable can be properly modelled if a large number of scenarios are generated following its distribution function. Thus, by using the mentioned truncated Gaussian distribution, a large number of scenarios for the initial SOC of the PEV are constructed. However, the generated scenarios have to be combined with the measured data available, in other words, one need an initial SOC of the PEV per day in order to maintain the coherency of the model. It is realistic to assume that raw data available usually span for one year (although large amount of data could be considered without any problem), so, it is suitable to reduce the number of scenarios generated to 365, in order to

combine them with the daily weather data and, thus, generate daily profiles to be simulated in the HEM problem. To that end, the k-medoids method is performed for only the initial SOC of the PEV (1st cluster). Intuitively, the total number of clusters is fixed in this stage and equal to the total days for which one has data (365 in our case). Then, the reduced scenarios are randomly combined with the available historical data and, jointly, are represented by means of representative days (2nd cluster), which serve as input of the optimization problem (see Fig. 3). To randomly combine the concerned profiles, a simple heuristic approach is followed. Firstly, the different days for which one has measured data are consecutively labelled, then, a random number from 1 to 365 is generated and assigned to each initial SOC of the PEV. Needless to say that if historical data about the initial SOC of the PEV were available, they can be treated as the other unknown parameters (solar irradiation or ambient temperature). For the sake of clarify, the whole procedure considered for representing the solar irradiation, ambient temperature and initial SOC of the PEV by means of representative days is summarized in Fig. 4.

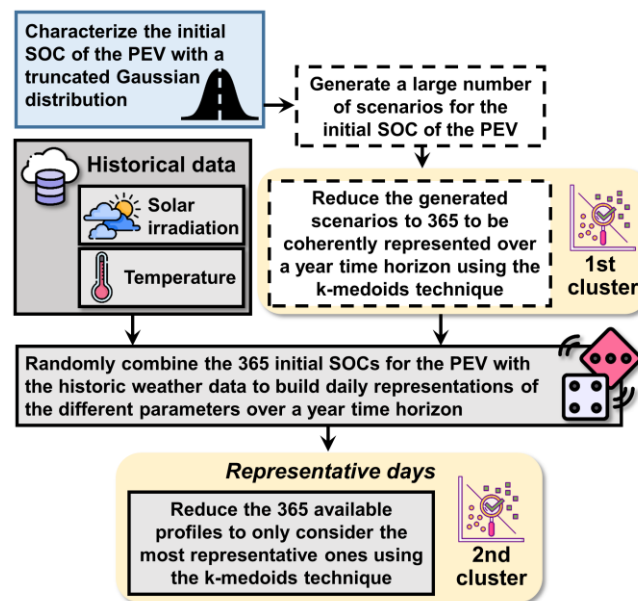


Fig. 4 - Flowchart of the procedure considered for representing the solar irradiation, ambient temperature and initial SOC of the PEV by means of representative days

4. Mathematical formulation of the planning problem

In this section, mathematical formulation of the developed optimal housing electrification system design for the dwelling described in Section 2 and Fig. 1 is presented and explained.

4.1.- Objective function

The developed optimal planning tool aims at reducing the total net present cost of the project through its estimated lifetime. To properly evaluate this aspect, different costs have to be calculated over different time horizons. Thus, it is assumed that the project incurs in capital yearly and daily costs. Thereby, the objective function for the developed sizing problem is given by:

$$\min_{\Phi} K + \sum_{\forall y \in \mathcal{Y}} \{(1+r)^{y-1} \cdot [Y_y + \sum_{\forall r \in \mathcal{R}} \{\omega_r \cdot D_r\}]\} \quad (1)$$

where Φ is the vector of decision variables, defined in this case as:

$$\Phi = \left\{ \begin{array}{l} \bar{p}^i, \bar{\varepsilon}^{\text{BES}}, p_{r|t}^j, \varepsilon_{r|t}^{ii}, u_{r|t}^{jj}, \theta_{r|t}^{iii} \\ u_{r|t}^{\text{App,d,k}}, \text{on}_{r|t}^{\text{App,d,k}}, \text{off}_{r|t}^{\text{App,d,k}}, z_{r|t} \end{array} \right\}; \forall r \in \mathcal{R}, \forall t \in \mathcal{T}, \forall i \in \{\text{DEG; PV}\}, \forall j \in$$

\{\text{DEG; PV; BES, ch; BES, dch; PEV, ch; PEV, dch; HVAC, h; HVAC, c; EWH}\}, \forall ii \in

\{\text{BES; PEV}\}, \forall jj \in

\{\text{DEG; BES, ch; BES, dch; PEV, ch; PEV, dch; HVAC, h; HVAC, c}\}, \forall iii \in

\{\text{air, in; w, h}\}, \forall k \in \mathcal{K} \quad (2)

In (1), different project costs are evaluated over different time scales. Capital costs (K) are referred to those expenditures in which the project incurs due to components purchase, installation, delivery, converter interface (if needed) and balance of plant. Thereby, such kind of inversions are undertaken once during the project lifetime (at the beginning of it assuming that all the components are installed at 1st year). Considering the home system layout described in Fig. 1, the capital costs of the electrification problem are given by:

$$K = \bar{p}^{\text{DEG}} \kappa^{\text{DEG}} + \bar{p}^{\text{PV}} (\kappa^{\text{PV}} + 1.1 \cdot 10^3 \cdot \kappa^{\text{Inv}}) + \bar{\varepsilon}^{\text{BES}} \kappa^{\text{BES}} \quad (3)$$

In (3), it has been considered that solar inverter is sized 10% higher than PV array capacity [12]; also, costs associated with the batteries charging controller have been included in the capital cost of the BES, for simplicity.

The yearly costs (Y) are referred to the operation, maintenance and replacement of the devices. The operation and maintenance expenditures of the assets are considered fixed and derived from the normal operation of the components. On the other hand, the project only incurs on replacement costs when a device has surpassed its expected lifetime and needs to be replaced. For example, assuming that all the assets are purchased at the 1st year of the project lifetime, if a component has an expected lifetime of 10 years, the yearly costs should contemplate the replacement of such device at 11th year. This way, the yearly costs are evaluated once per year and are defined as follows:

$$Y_y = \bar{p}^{\text{DEG}} \cdot (\gamma_y^{\text{DEG}} \nu^{\text{DEG}} + \mu^{\text{DEG}}) + \bar{p}^{\text{PV}} \cdot (\gamma_y^{\text{PV}} \nu^{\text{PV}} + 1.1 \cdot 10^3 \cdot \gamma_y^{\text{Inv}} \nu^{\text{Inv}} + \mu^{\text{PV}}) + \bar{\varepsilon}^{\text{BES}} \cdot (\gamma_y^{\text{BES}} \nu^{\text{BES}} + \mu^{\text{BES}}); \forall y \in \mathcal{Y} \quad (4)$$

In (4), the parameter γ 's are introduced in order to only consider the replacement costs of the different devices when their expected lifetime has been surpassed and need to be replaced.

Finally, daily costs (D) correspond to the expenditures due to fuel consumption, lifetime reduction and carbon tax of the DEG and are given by:

$$D_r = \sum_{\forall t \in \mathcal{T}} \left\{ \frac{\nu^{\text{DEG}} \cdot \Delta \tau}{T^{\text{DEG}}} \cdot u_{r|t}^{\text{DEG}} + \sigma(y) \cdot f_{r|t}^{\text{DEG}} \cdot (\lambda^{\text{DEG}} + 10^{-3} \cdot \varphi^{\text{DEG}} \cdot \rho^{\text{DEG}}) \right\}; \forall r \in \mathcal{R} \quad (5)$$

In the expression (5), f^{DEG} is the fuel consumption of the DEG. Occasionally, the diesel consumption of DEGs is represented by a quadratic function of the power given by (e.g. see [35]). However, as pointed out in [18], it can be approximated by a linear function for small-scale devices, as follows:

$$f_{r|t}^{\text{DEG}} = \beta^{\text{DEG}} \cdot \underbrace{u_{r|t}^{\text{DEG}} \cdot \bar{p}^{\text{DEG}}}_{z_{r|t}} + \alpha^{\text{DEG}} \cdot p_{r|t}^{\text{DEG}}; \forall r \in \mathcal{R}, \forall t \in \mathcal{T} \quad (6)$$

It is worth commenting that the function σ is introduced in (1) in order to consider home demand variations during the project lifetime. Indeed, growing temperature besides the emergence of very efficient appliances, lead to think that fuel consumption may be reduced in future. Nevertheless, this function can be defined as considered. Replacement costs of the DEG have been included in (5) due to the expected lifetime of this device is normally given in working hours by manufactures (first term in (5)), consequently, they cannot be properly evaluated in (4). On the other hand, the dummy variable z has been included in order to avoid bilinear terms [36]. The consideration of this variable requires to include the following set of constraints in the problem:

$$\bar{p}^{\text{DEG}} - L(1 - u_{r|t}^{\text{DEG}}) \leq z_{r|t} \leq \bar{p}^{\text{DEG}} + L(1 - u_{r|t}^{\text{DEG}}); \forall r \in \mathcal{R}, \forall t \in \mathcal{T} \quad (7)$$

$$-L \cdot u_{r|t}^{\text{DEG}} \leq z_{r|t} \leq L \cdot u_{r|t}^{\text{DEG}}; \forall r \in \mathcal{R}, \forall t \in \mathcal{T} \quad (8)$$

It is worth noting that maintenance costs of batteries and solar panels have not been considered in (5), since it is assumed that these spending are negligible in comparison with fuel expenditures, which is a reasonable assumption in HEM formulations [20].

4.2.- Formulation of the HEM sub-problem

As commented, the developed planning **framework** involves a HEM sub-problem which is required to properly evaluate the project daily costs. The formulation of this problem is a modified version of other related works [5, 20, 21].

4.2.1.- Modelling the DEG

Considering that ramp constraints of the DEG may be neglected (assuming a sufficiently large time step and a small-scale DEG unit [37]), the DEG can be modelled by the constraint (9), which upper and lower bounds the power given by this device.

$$u_{r|t}^{\text{DEG}} \underline{p}^{\text{DEG}} \leq p_{r|t}^{\text{DEG}} \leq \underbrace{u_{r|t}^{\text{DEG}} \bar{p}^{\text{DEG}}}_{z_{r|t}}; \forall r \in \mathcal{R}, \forall t \in \mathcal{T} \quad (9)$$

4.2.2.- Modelling the PV array

A HEM system normally determine the day-ahead available PV generation on the basis of weather forecast. Let us assume that the representative days generated following the procedure described in Fig. 4 serve as forecasts inputs of the concerned HEM problem. This way, the instantaneous maximum power that a PV array can give can be calculated as follows [38]:

$$\phi_{r|t}^{\text{PV}} = \bar{p}^{\text{PV}} \vartheta_{r|t} \cdot \{0.8 + 0.024(\theta_{r|t}^{\text{air,in}} + \vartheta_{r|t} \cdot [33.8 - 37.5\eta^{\text{PV}}] - 25)\}; \forall r \in \mathcal{R}, \forall t \in \mathcal{T} \quad (10)$$

In (10), it is assumed that solar irradiation has been previously corrected due to panels tilt angle [39]. In this work, a fixed tilt angle has been considered, which is a common situation in most dwellings. However, the equation (10) does not consider functional limits. In other words, the equation (10) may yield values higher than \bar{p}^{PV} , which is not realistic since, in practise, the inverter limits this value to only admit light overloads over the PV system capacity. In order to reflect this restriction, the constraint (11) has to be added.

$$0 \leq p_{r|t}^{\text{PV}} \leq \begin{cases} \phi_{r|t}^{\text{PV}}, & \text{if } \phi_{r|t}^{\text{PV}} \leq 1.1 \cdot \bar{p}^{\text{PV}} \\ 1.1 \cdot \bar{p}^{\text{PV}}, & \text{o. w.} \end{cases}; \forall r \in \mathcal{R}, \forall t \in \mathcal{T} \quad (11)$$

It is worth mentioning that other renewable-based sources could be straightforward modelled. For example, if the considered home incorporates wind-based generators, the expression (10) should be replaced by the well-known speed-power modelling of wind turbines [38], which provides the expected power output of a wind turbine as a function of the wind speed.

4.2.3.- Modelling the BES and PEV

Both BES and PEV are stated as electro-chemical storage models, with only some functional differences between both formulations. This way, the BES and PEV can be broadly modelled by the equations (12)-(15).

$$0 \leq p_{r|t}^{i,j} \leq u_{r|t}^{i,j} \bar{p}^i; \forall r \in \mathcal{R}, \forall t \in \mathcal{T}, \forall i \in \{\text{BES}; \text{PEV}\}, \forall j \in \{\text{ch}; \text{dch}\} \quad (12)$$

$$(1 - \text{DOD}^i) \cdot \bar{\varepsilon}^i \leq \varepsilon_{r|t}^i \leq \bar{\varepsilon}^i; \forall r \in \mathcal{R}, \forall t \in \mathcal{T}, \forall i \in \{\text{BES}; \text{PEV}\} \quad (13)$$

$$\varepsilon_{r|t}^i = \varepsilon_{r|t-1}^i + \Delta\tau \cdot \left(p_{r|t}^{i,\text{ch}} \eta^i - \frac{p_{r|t}^{i,\text{dch}}}{\eta^i} \right) \forall r \in \mathcal{R}, \forall t \in \mathcal{T} \setminus t > 1, \forall i \in \{\text{BES}; \text{PEV}\} \quad (14)$$

$$\sum_{j \in \{\text{ch}; \text{dch}\}} \{u_{r|t}^{i,j}\} \leq 1; \forall r \in \mathcal{R}, \forall t \in \mathcal{T}, \forall i \in \{\text{BES}; \text{PEV}\} \quad (15)$$

The equation (12) upper bounds the instantaneous power exchanged with the home to rated values. The energy stored has to be limited by the allowed depth-of-discharge and nominal capacity, which is contemplated by the constrain (13). The equation (14) models the instantaneous SOC. Finally, the constraint (15) forces to charging and discharging modes to be complementary processes.

In HEM problems, the initial SOC of the BES has to be fixed [5], since the equation (14) is not defined for $t = 1$. Generally, it is assumed that the BES is fully charged at the beginning of the evaluating period, which is a reasonable assumption if one forces the BES to be also fully charged at the end of the time horizon. This behaviour is modelled by the constraint (16).

$$\varepsilon_{r|1}^{\text{BES}} = \varepsilon_{r|\mathcal{T}}^{\text{BES}} = \bar{\varepsilon}^{\text{BES}}; \forall r \in \mathcal{R} \quad (16)$$

On the other hand, modelling the PEV presents some particularities. Firstly, on-board storage system of PEV is not available during some hours of the day when it is assumed that the PEV is not parked at home. This restriction is modelled by the constraint (17). Secondly, it is assumed that home inhabitants desire to get the PEV fully charge at its departure time, which is achieved by imposing the equation (18).

$$\sum_{t=\hat{t}}^{t=\hat{t}} \sum_{i \in \{\text{ch}; \text{dch}\}} \{u_{r|t}^{\text{PEV},i}\} = 0; \forall r \in \mathcal{R} \quad (17)$$

$$\varepsilon_{r|\hat{t}}^{\text{PEV}} = \bar{\varepsilon}^{\text{PEV}}; \forall r \in \mathcal{R} \quad (18)$$

4.2.4.- Modelling the deferrable appliances

Conventionally, operating principle of the deferrable appliances must a series of principles, which are modelled by the set of constraints (19)-(21) [20].

$$\text{on}_{r|t}^{\text{App,d,k}} - \text{off}_{r|t}^{\text{App,d,k}} = u_{r|t}^{\text{App,d,k}} - u_{r|t-1}^{\text{App,d,k}}; \forall r \in \mathcal{R}, \forall t \in \mathcal{T} \setminus t > 1, \forall k \in \mathcal{K} \quad (19)$$

$$\sum_{\forall t \in \mathcal{T}} \left\{ \text{on}_{r|t}^{\text{App,d,k}} \right\} = 1; \forall r \in \mathcal{R}, \forall k \in \mathcal{K} \quad (20)$$

$$\sum_{\forall t \in \Omega^k} \left\{ u_{r|t}^{\text{App,d,k}} \right\} = \delta^k; \forall r \in \mathcal{R}, \forall k \in \mathcal{K} \quad (21)$$

The constraint (19) imposes that the deferrable appliances are operated in consecutive time slots. Each deferrable appliance can only be activated once during the considered time horizon, which is achieved by imposing the constraint (20). Finally, the equation (21) forces to complete the duty cycle of the deferrable appliances within allowed time windows (Ω).

4.2.5.- Modelling the thermostatically controlled appliances

Dynamic behaviour of thermal inertia is typically modelled by differential equations which, under some plausible assumptions, can be linearized [20, 40]. Thereby, the instantaneous home inside and hot water temperatures can be modelled by the equations (22) and (23)-(24), respectively.

$$\theta_{r|t}^{\text{air,in}} = \Delta\tau \left[\left(1 - \frac{1}{10^3 \cdot M^{\text{air,in}} \cdot C^{\text{air,in}} \cdot R^{\text{build}}} \right) \theta_{r|t-1}^{\text{air,in}} + \frac{1}{10^3 \cdot M^{\text{air,in}} \cdot C^{\text{air,in}} \cdot R^{\text{build}}} \theta_{r|t-1}^{\text{air,out}} + \frac{(p_{r|t-1}^{\text{HVAC,h}} - p_{r|t-1}^{\text{HVAC,c}})}{0.000277 \cdot M^{\text{air,in}} \cdot C^{\text{air,in}}} \text{COP}^{\text{HVAC}} \right]; \forall r \in \mathcal{R}, \forall t \in \mathcal{T} \setminus t > 1 \quad (22)$$

$$\theta_{r|t+1}^{\text{w,h}} = \theta_{r|t}^{\text{air,in}} + p_{r|t}^{\text{EWH}} \eta^{\text{EWH}} C^{\text{w,h}} - (\theta_{r|t}^{\text{air,in}} - \theta_{r|t}^{\text{w,h}}) e^{-\frac{\Delta\tau}{R^{\text{w,h}} C^{\text{w,h}}}}; \forall r \in \mathcal{R}, \forall t \in \mathcal{T} \setminus t < \mathcal{T}, v_{r|t}^{\text{w,h}} = 0 \quad (23)$$

$$\theta_{r|t+1}^{\text{w,h}} = \frac{\theta_{r|t}^{\text{w,h}} (v^{\text{EWH}} - v_{r|t}^{\text{w,h}}) + \theta_{r|t}^{\text{w,c}} v_{r|t}^{\text{w,h}}}{v^{\text{EWH}}}; \forall r \in \mathcal{R}, \forall t \in \mathcal{T} \setminus t < \mathcal{T}, v_{r|t}^{\text{w,h}} > 0 \quad (24)$$

Similar to the initial SOC of the BES, the inside and hot water temperatures at the beginning of the time horizon have been fixed. In this case, let us assume that both parameters are equal to the desired set-point at $t = 1$. In order to maintain the model coherency, these temperatures are forced to be equal to their respective set-points at the

end of the evaluating period. These two restrictions are imposed by the constraints (25) and (26).

$$\theta_{r|1}^{\text{air,in}} = \theta_{r|\mathcal{T}}^{\text{air,in}} = \theta^{\text{HVAC,sp}}; \forall r \in \mathcal{R} \quad (25)$$

$$\theta_{r|1}^{\text{w,h}} = \theta_{r|\mathcal{T}}^{\text{w,h}} = \theta^{\text{EWH,sp}}; \forall r \in \mathcal{R} \quad (26)$$

It is assumed that home inhabitants desire certain comfort levels. In the case of the HVAC system, it is devoted to maintain the home inside temperature within acceptable limits. Nevertheless, in order to avoid a repeatedly operation of this device, a dead-band is included. Under this premises, the inside temperature is upper and lower bounded by the constraint (27). In the case of the EWH, the hot water temperature is allowed to vary from the desired set-point to a setting upper bounded (which is considered for security reasons [20]), by imposing the constraint (28).

$$\theta^{\text{HVAC,sp}} - \theta^{\text{HVAC,db}} \leq \theta_{r|t}^{\text{air,in}} \leq \theta^{\text{HVAC,sp}} + \theta^{\text{HVAC,db}}; \forall r \in \mathcal{R}, \forall t \in \mathcal{T} \quad (27)$$

$$\theta^{\text{w,h,sp}} \leq \theta_{r|t}^{\text{w,h}} \leq \bar{\theta}^{\text{w,h}}; \forall r \in \mathcal{R}, \forall t \in \mathcal{T} \quad (28)$$

Thermostatically controlled appliances modelling is completed by including the constraints (29)-(30) and (31). The formers contemplate that power consumption of both HVAC system and EWH cannot be higher than rated values; while the later avoids an abnormal operation of the HVAC system, by imposing that both heating and cooling modes are complementary.

$$p_{r|t}^{\text{HVAC},i} \leq u_{r|t}^{\text{HVAC},i} \bar{p}^{\text{HVAC}}; \forall r \in \mathcal{R}, \forall t \in \mathcal{T}, \forall i \in \{h, c\} \quad (29)$$

$$0 \leq p_{r|t}^{\text{EWH}} \leq \bar{p}^{\text{EWH}}; \forall r \in \mathcal{R}, \forall t \in \mathcal{T} \quad (30)$$

$$\sum_{i \in \{h, c\}} \{u_{r|t}^{\text{HVAC},i}\} \leq 1; \forall r \in \mathcal{R}, \forall t \in \mathcal{T} \quad (31)$$

4.2.6.- Home balance

Finally, a home energy balance has to be imposed (32). In this case, non-served energy has not been contemplated assuming that total home demand could be eventually supplied by means of the DEG.

$$p_{r|t}^{\text{DEG}} + p_{r|t}^{\text{PV}} + \sum_{\forall i \in \{\text{BES}; \text{EV}\}} \{p_{r|t}^{j, \text{dch}}\} = \sum_{\forall i \in \{\text{BES}; \text{EV}\}} \{p_{r|t}^{j, \text{ch}}\} + p_{r|t}^{\text{App, nd}} + \sum_{\forall i \in \{\text{h}; \text{c}\}} \{p_{r|t}^{\text{HVAC}, i}\} + p_{r|t}^{\text{EWH}} + \sum_{\forall k \in \mathcal{K}} \{u_{r|t}^{\text{App, d}, j} \bar{p}^{\text{App, d}, j}\}; \forall r \in \mathcal{R}, \forall t \in \mathcal{T} \quad (32)$$

4.3.- Project limits

Planning tools should take into account some limits that are determined by either user-imposed restrictions or constructive aspects. In that sense, it is assumed that initial budget is limited to some quantity that home users are willing to undertake. This restriction is reflected by the constraint (33).

$$K \leq Y \quad (33)$$

On the other hand, equipment sizing should be also limited as this aspect may be constrained by constructive or environmental aspects. For example, PV capacity may be bounded by the available roof surface, which can indirectly impose the maximum numbers of PV panels that could be installed. This limitation is modelled in the developed problem by imposing the set of constraints (34)-(35).

$$\bar{p}^i \leq \Psi^i; \forall i \in \{\text{DEG}; \text{PV}\} \quad (34)$$

$$\bar{\varepsilon}^{\text{BES}} \leq \Psi^{\text{BES}} \quad (35)$$

5. Case study

5.1.- Input data

The value of the different parameters used in simulations are reported in Table 1 and have been collected from various references [5, 12, 13, 18, 20, 21]. The data related with thermal inertia of the building and EWH have been taken from [20] and are reported in Table 2. Table 3 shows the characteristics of the truncated Gaussian distribution function used to generate initial SOCs of the PEV for simulations [21]. The different costs and expected lifetimes of PV panels, BES and DEG are reported in Tables 4-6, respectively. The different features of the considered deferrable appliances are showed in Table 7. The estimated project lifetime has been taken equal to 25 years and the inflation rate equal to

0.27 %. For simplicity, it is assumed that the PEV arrives at 19:00 h and leaves the home at 7:00 h. Therefore, in order to fully exploit the PEV capabilities, the HEM sub-problem has been solved over a 24-hrs time horizon with 30-min resolution (19:00-18:30 h).

Table 1 - The value of the parameters used in simulations [5, 12, 13, 18, 20, 21]

Parameter	Value	Parameter	Value
$\bar{p}^{\text{BES}}/\bar{p}^{\text{PEV}}$	1.5/3 kW	$\text{COP}^{\text{HVAC}}/$	1.2
$\eta^{\text{BES}}/\eta^{\text{PEV}}$	0.98/0.98	\bar{v}^{EWH}	50 gal
$\text{DOD}^{\text{BES}}/\text{DOD}^{\text{PEV}}$	0.6/0.8	$\theta^{\text{HVAC,sp}}/\theta^{\text{HVAC,db}}$	23/0.5 °C
$\bar{\varepsilon}^{\text{PEV}}$	22 kWh	$\theta^{\text{w,h,sp}}/\bar{\theta}^{\text{w,h}}$	45/60 °C
η^{PV}	0.167	$\theta^{\text{w,c}}$	10 °C
p^{DEG}	0.1 kW	Υ	7,000 \$
$\bar{p}^{\text{HVAC}}/\bar{p}^{\text{EWH}}$	2/2.1 kW	$\Psi^{\text{DEG}}/\Psi^{\text{PV}}$	7/2.5 kW
η^{EWH}	0.9	Ψ^{BES}	3 kWh

Table 2 - Thermal characteristics of the building and EWH [20]

Parameter	Value
$M^{\text{air,in}}$	1,778.4 kg
$C^{\text{air,in}}$	1.01 kJ/(kg · °C)
R^{build}	$3.2 \cdot 10^{-6}$ J/°C
$R^{\text{w,h}}$	863.4 °C/kWh
$C^{\text{w,h}}$	1.52 °C/kW

Table 3 - Characteristics of the truncated Gaussian distribution used for generating initial SOC's for the PEV [21]

Mean	Std. dev.	Min.	Max.
0.5	0.25	0.2	0.95

Table 4 - Cost data of PV panels and solar inverter [12, 13]

Cost	PV panels	Inverter
Capital cost	1,210 \$/kW	0.31 \$/W
Replacement cost	484 \$/kW	0.31 \$/W
Maintenance cost	15 \$/kW-yr	--
Lifetime	25 years	12 years

Table 5 - Cost data of the BES [5, 13]

Capital cost	300 \$/kWh
Replacement cost	300 \$/kWh
Maintenance cost	2.75 \$/kWh-yr
Lifetime	12 years

Table 6 - Cost data of the DEG [13, 18, 41]

Capital cost	340 \$/kW
Replacement cost	340 \$/kW
Maintenance cost	3.5 \$/kW-yr
Lifetime	30,000 hours
$\alpha^{\text{DEG}}/\beta^{\text{DEG}}$	0.08415/0.246 litres/kW
λ^{DEG}	0.2 \$/litre
ρ^{DEG}	2.4 kg/litre
φ^{DEG}	20 \$/ton

Table 7 - Characteristics of the deferrable appliances

Appliance	Rated power (kW)	Time window	δ
Washing machine	1.5	1:00-18:30 h	3
Dishwasher	2.5	7:00-16:00 h	4

Measured data for solar irradiation and ambient temperature have been taken from [42] for the city of Madrid through 2016. If other renewable-based generators were aimed to be analysed, one can recur to other public database. For instance, historical wind speed measurements are available in [43]. It has been considered that solar panels are installed with a fixed tilt angle equal to 40°. This way, data collected in [42] has been corrected using [39, eq. 2], neglecting the effect of in-plane diffuse irradiance and irradiance due to ground reflection. The available data for the year 2016 has been reduced to 14 scenarios (see Fig. 5) using the k-medoids technique. As commented, the total number of scenarios has been set by observing the value of some helpful indicators like the total sum of distances and Davies Bouldin index. In this sense, the same procedure described in [5] has been followed in this paper, which basically finds the lowest clustering number beyond which the total sum of distances is not further reduced. This value indicates that the dissimilarity of the members within a cluster is not notably reduced by increasing the number of sets. After that, the Davies Bouldin index is observed. This index gives an idea of the dissimilarity among clusters, so that a low value of this indicator is desirable. Thus, starting from the value beyond which the total sum of distances is not reduced, the clustering number with the lowest Davies Bouldin index is selected.

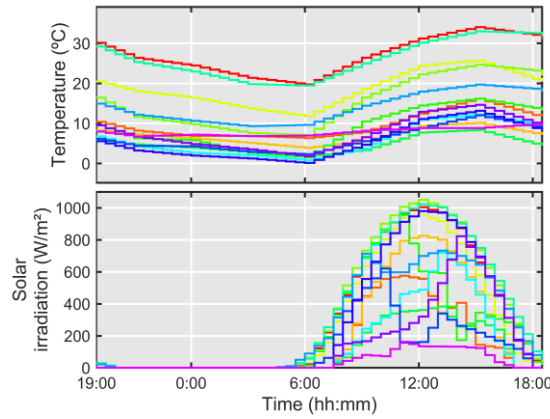


Fig. 5 - The 14 representative days taken for simulations

The non-deferrable appliances and hot water consumption has been taken fixed through the project lifetime, assuming that it is mainly due to repetitive inhabitants' routines (see Fig. 6). On the other hand, it is considered a fuel consumption reduction by 2% during the project lifetime. This way, the function σ has been built such as it is depicted in Fig. 7.

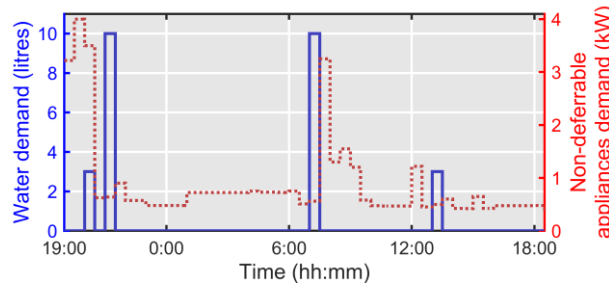


Fig. 6 - Non-deferrable appliances and hot water consumption

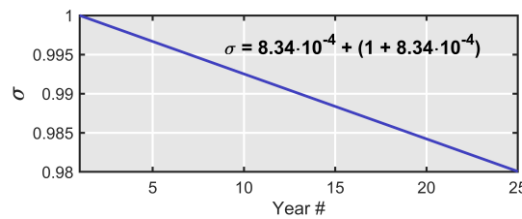


Fig. 7 - The value of the function σ through the project lifetime

5.2.- Configurations and scenarios analysed

In order to comprehensively analyse the home system described in Section 2, different layouts have been considered whose characteristics are summarized in Table 8. On the other hand, different demand-side management strategies have been also implemented in combination with the different layouts analysed (see Table 9). In the case of total

inflexible demand, it is assumed that the deferrable appliances cannot be controlled by the HEM system and are always activated at the beginning of their time windows (e.g. the dishwasher works from 7:00-8:30 h every day). In total, 16 scenarios have been analysed (4 layouts in combination with 4 demand-side strategies).

Table 8 - The different home layouts analysed

Generation units	Configuration #			
	1	2	3	4
DEG	Yes	Yes	Yes	Yes
BES	No	Yes	No	Yes
PV	No	No	Yes	Yes

Table 9 - The different demand-side management strategies adopted

Capability exploited	Demand-side strategy #			
	A	B	C	D
Flexible demand	No	Yes	No	Yes
V2H	No	No	Yes	Yes

5.3.- Results

Throughout this section, various simulations are carried out and several results are presented and discussed. The results are organized in various subsections, to make easier their analysis.

5.3.1.- Impact of the demand side management and V2H capability on the electrification project cost

The most important aspect which determines the viability of an electrification project is its total cost through its estimated lifetime. The introduced optimal electrification framework allows to straightforward evaluate it by simply observing the objective function (1). Fig. 8 compares the total project costs in different scenarios. As seen, the highest cost was observed when the configuration 1 was considered. In contrast, the total project cost was reduced by ~54% by opting for the Configuration 4. It is also worth observing that the configuration 2 is quite profitable despite no PV capacity is installed. On the other hand, one can check that the total project cost may be reduced up to ~21.2% and ~25.73% by adopting the strategies B and C, respectively. Nevertheless, the lowest

project expenditures were obtained with the strategy D (up to ~41.5% w.r.t the strategy A). This result was expected since this strategy jointly exploit demand flexibility and V2H capabilities, **this way, a great degree of freedom is provided to the HEM scheduling problem.**

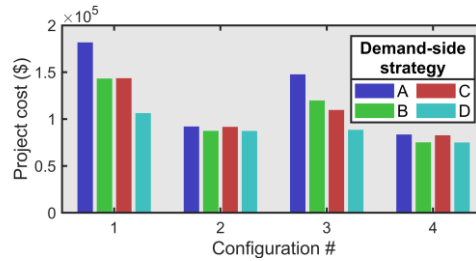


Fig. 8 - Total project cost with different layouts and demand-side management strategies

By the results reported in Fig. 8, it seems clear that disregarding demand-side management notably overestimates the project cost. Nevertheless, the developed optimization framework allows to extract other useful results, which are discussed in following sections.

5.3.2.- Home layout sizing

One important concern of home users is how the different demand-side strategies may help to reduce the size of some components (especially DEG). Fig. 9 shows the layout sizing results for different cases. As observed, the configurations 2 and 4 allow to drastically reduce the backup requirements of the home system. **Specifically**, DEG rated power can be reduced up to ~23% by opting for these two configurations w.r.t. the configuration 1. This result confirms that storage systems contribute more notably to reduce backup requirements than the PV generation. Indeed, with the configuration 3 the DEG sizing was **just** reduced by ~1.5%.

Comparing the different demand-side management strategies, one can clearly note that the strategies B and D had a very significant effect on DEG sizing reduction. Thereby, DEG optimal rated power may be reduced up to ~38.6% by adopting the strategy D instead of A. This fact put on manifest that flexible demand contributes more significantly

than the V2H capability to reduce backup requirements in this case. To explain it, let us analyse the Fig. 10, where the scheduling results for a representative day with the configurations 3B and 3C are depicted. As observed, in the latter case the DEG was forced to be sized according to the peak demand value, which is largely produced by PEV charging and washing machine scheduling at the same time during dawn. Indeed, when V2H capability is enabled, the electric vehicle tends to be highly charged during evening to take advantage of the V2H capacity during night. On the other hand, when demand flexibility is exploited, washing machine is scheduled during evening, avoiding peak power consumption about 1:00 h.

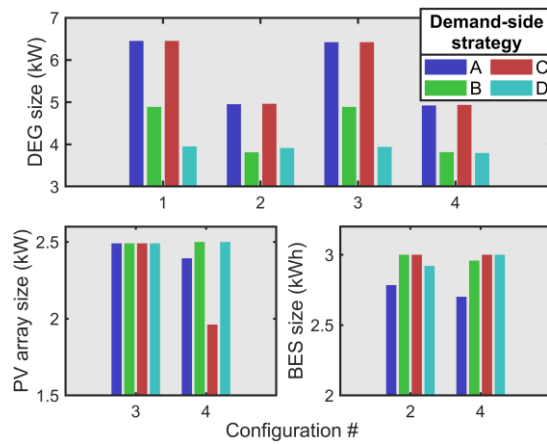


Fig. 9 - Components sizing comparison with different layouts and demand-side management strategies

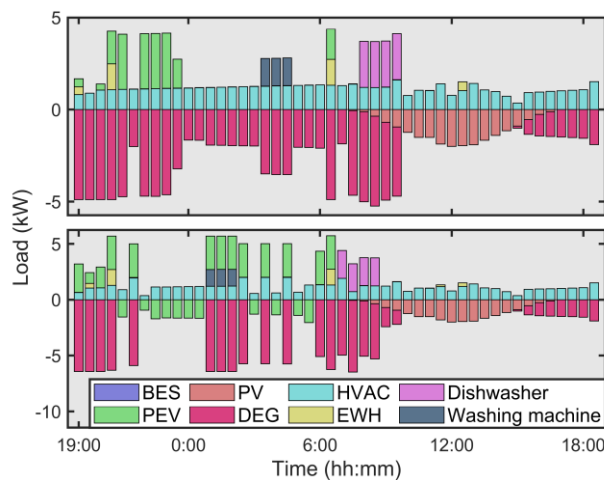


Fig. 10 - Scheduling results for a representative day with configurations 3B (top) and 3C (bottom). In this figure, negative values mean ‘to-home’ flow direction (generation)

Regarding the PV array, it is normally sized according to the maximum allowable capacity (2.5 kW). However, with the configuration 4 and demand-side strategy C, the PV capacity was determined to be ~1.9 kW. To analyse this result, let us compare the scheduling results with the configuration 4 and strategies B and C in Fig. 11. As seen in this figure, the deferrable appliances were scheduled during midday when the strategy B is adopted, in order to take advantage of large PV generation during these hours. On the other hand, as no flexibility is allowed with the strategy C, both deferrable appliances are operated during dawn and early morning. Under these circumstances, the demand that PV panels have to cover is much lower and, consequently, the PV sizing can be lowered. Last, regarding the BES sizing, this component was normally sized at its maximum allowable value or close to it, regardless the configuration or demand-side strategy adopted.

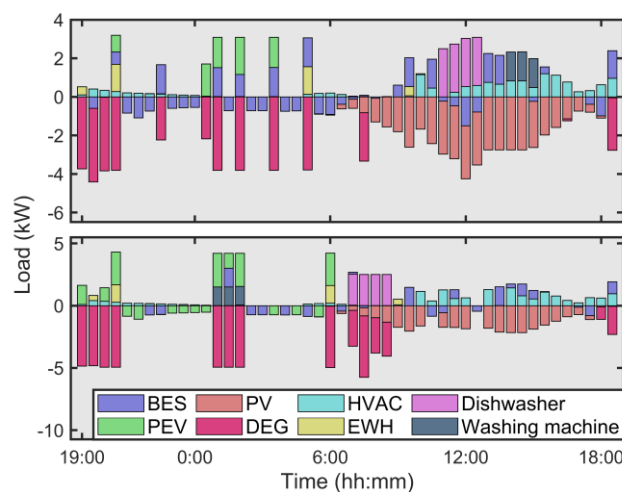


Fig. 11 - Scheduling results for a representative day with configurations 4B (top) and 4C (bottom). In this figure, negative values mean 'to-home' flow direction (generation)

5.3.3.- V2H exploitation

The degree in which the electric vehicle is exploited in discharging mode (V2H mode), may influence on the decision of the home owners to undertake some monetary inversions on auxiliary equipment, as for example, a bidirectional charger. Similarly, the necessity of installing a BES bank may be questionable if the electric vehicle actual

provides sufficient storage capability. In this sense, it is worth observing that considering the V2H capability of the PEV has a much more significant impact on the total project cost with the configuration 3. This evidence leads us to think that the V2H capability is further exploited when the BES is not installed. This is logic since in the case of no deploying a BES system, the PEV plays the role of the storage facility. Indeed, this evidence is confirmed in Fig. 12, where total energy delivered by PEV through project lifetime is compared for different cases. As seen, V2H capability is further exploited (up to ~46% more) with the layouts 1 and 3. This behaviour is further illustrated in Fig. 13, where scheduling results for a representative day with the configurations 2C and 3C are compared. In this figure one can observe that the PEV is mainly operated as a pure load while storage capacity is largely provided by the BES with the configuration 2C. In contrast, the PEV considerably provided storage capacity with the configuration 3C.

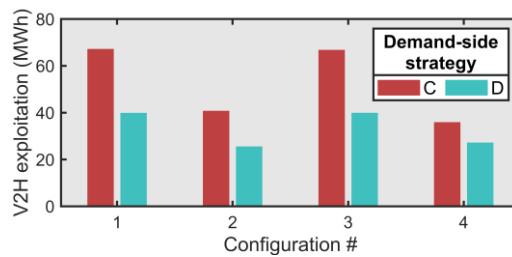


Fig. 12 - V2H exploitation through project lifetime with different layouts and demand-side management strategies

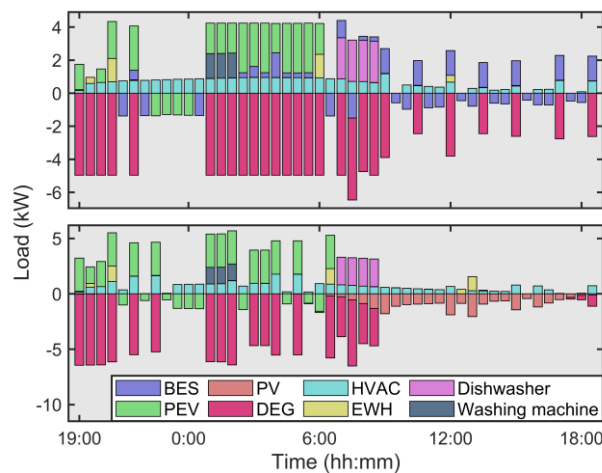


Fig. 13 - Scheduling results for a representative day with configurations 2C (top) and 3C (bottom). In this figure, negative values mean ‘to-home’ flow direction (generation)

It remains to be analysed why the degree of V2H exploitation falls with the adoption of the strategy D w.r.t. to C (by ~40% on average). This fact is explained by the resulting DEG sizing for each case. Indeed, a higher backup capacity allows the PEV to be charged faster, as checked in Fig. 14, where the SOC of the PEV and the instantaneous backup generation are compared with the configurations 4C and 4D. Due to a faster charging-discharging capability, the V2H feature of the PEV can be further exploited, especially from 4:00-6:00 h since, as observed in Fig. 14, the PEV can be partially discharged during these time slots with the strategy C whereas it acts as a pure load with the demand-side strategy D. Therefore, one can conclude that the impact of the different demand-side strategies cannot be properly compared with different DEG sizing. In order to provide a further insight to this issue, we have compared the degree of V2H exploitation with the highest DEG size calculated (6.50 kW) and the comparison is shown in Fig. 15. As observed, the degree of V2H exploitation is not much different comparing the strategies C and D. Hence, it can be concluded that the flexibility on the demand does not notably affect the utilization of the storage capability of the PEV.

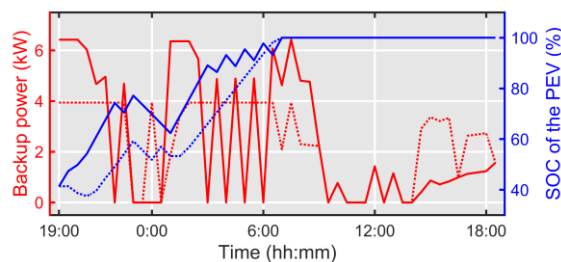


Fig. 14 - Comparison of the backup power and the SOC of the PEV with configurations 4C (continuous lines) and 4D (dotted lines)

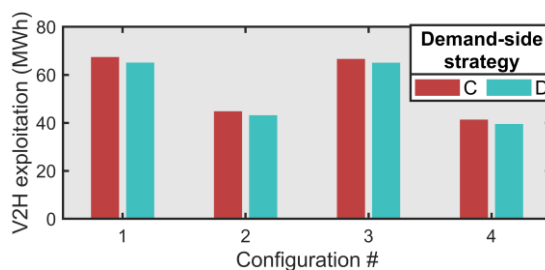


Fig. 15 - V2H exploitation through project lifetime with different layouts and demand-side management strategies. The results reported in this figure have been calculated with the same DEG size (6.50 kW)

5.3.4.- Impact of the demand-side strategies and V2H capability on the exploitation of renewable sources

Other crucial aspect for home users is the degree in which the renewable sources are exploited. This aspect may determine the monetary inversion dedicated to onsite renewable generators. Fig. 15 compares the use of the PV panels for each case (in percentage), the solar energy is further exploited with the configuration 4 and the strategies B and D. These results are expected since, as seen in Fig. 11, if flexible demand is enabled, the deferrable appliances are logically scheduled during those hours with high PV generation, in order to reduce the DEG use. On the other hand, deploying a BES system allows to effectively manage with PV generation. Indeed, as seen in Fig. 16 where the scheduling results with the configurations 3A and 4A, the batteries are largely discharged during evening and night, while during the central hours of the day, high PV generation is exploited to charge them. Otherwise, the home layout is unable to make a further usage of the all PV potential.

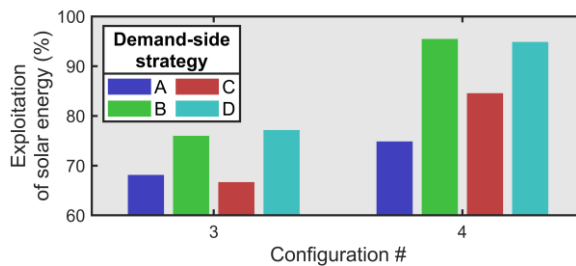


Fig. 15 - Exploitation of available solar energy with various configurations and demand-side strategies

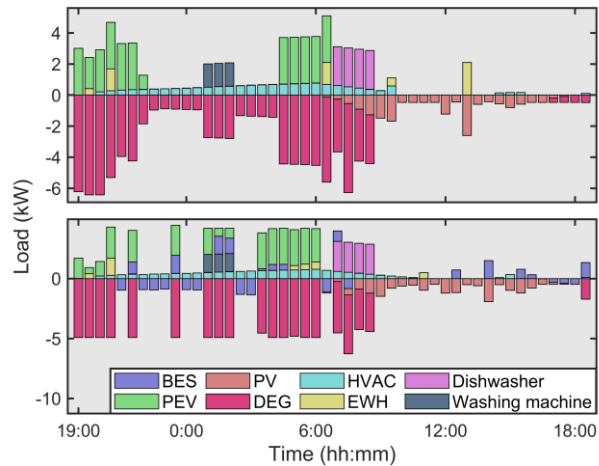


Fig. 16 - Scheduling results for a representative day with configurations 3A (top) and 4A (bottom). In this figure, negative values mean ‘to-home’ flow direction (generation)

5.3.5.- DEG-related results

The backup generator is a vital component for the optimal electrification of off-grid homes. It is necessary to meet the instantaneous demand during those hours with low PV penetration. At the same time, this device is responsible of the daily monetary expenditures due to fuel consumption and CO₂ emissions. In this sense, various relevant aspects related to the DEG are broadly presented in Fig. 17. As observed, the total fuel costs are quite proportional to the DEG sizing. Thus, the total expenditures dedicated to fuel consumption through the project lifetime can be reduced by ~58% comparing the layouts 1 and 4 and by ~42% comparing the strategies A and D. In contrast, this trend was not observed for the total hours that the DEG is operated through project lifetime. In this regard, it is shown that backup generation was less required with the strategy C (even with the strategy A in some cases) in comparison with adopting the strategies B and D. It means that, despite less backup requirements are necessary by adopting the strategies B or D, the DEG unit is operated during more hours. This fact should be taken into account since by adopting the strategies B and D the DEG unit could experience a faster ageing. Specifically, the total working hours of the DEG were reduced up to ~53% and ~31% with the home layout 4 and the demand-side strategy C.

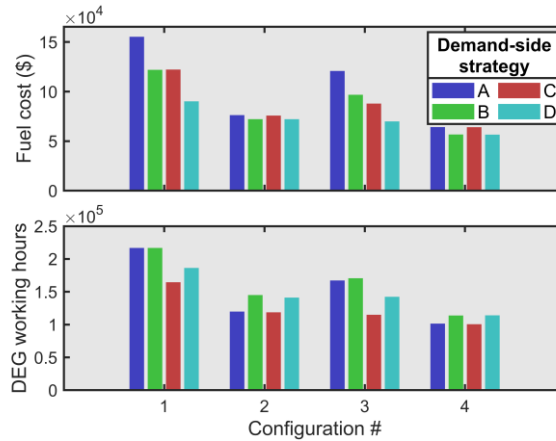


Fig. 17 - Total fuel cost (top) and DEG working hours (bottom) through project lifetime with different layouts and demand-side management strategies

5.3.6.- CO₂ emissions

Nowadays, environmental concerns suppose a crucial issue to be taken into account in any electrification project. For our home layout, the DEG supposes a CO₂ source and, consequently, its gas emissions are aimed to be reduced as much as possible. Nowadays, many countries penalize the pollutant emissions by taxing the kg of CO₂ delivered to the atmosphere [44]. Consequently, this aspect should be carefully studied in any energy system model. In our case, this aspect has been taken into account by including a fixed carbon tax in the daily costs, which is proportional to the diesel consumption. Fig. 18 compares the total CO₂ emissions through the project lifetime for various layouts and demand-side strategies. As expected, this result is quite proportional to the total fuel cost reported in Fig. 17. Thus, similar conclusions can be drawn.

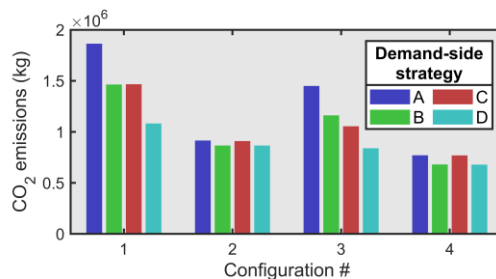


Fig. 17 - Total CO₂ emissions through project lifetime with different layouts and demand-side management strategies

6. Conclusions and future works

This work has presented an optimization framework for optimal electrification of off-grid dwellings, which allows to consider and analyse the impact of different demand-side management strategies such as deferrable appliances and vehicle-to-home capabilities. This problem has been formulated as a multi-time scale approach in which different costs are evaluated over different time scales. A Home Energy Management sub-problem is included in order to analyse daily fuel costs and carbon tax of the Diesel generator unit. Besides the total project cost and optimal home layout, it has been shown that the developed methodology also allows to extract other useful results.

Various simulations have been carried out on a benchmark stand-alone home system and different results have been presented and discussed. Various conclusions and findings have been drawn from the analysis of the results obtained throughout previous sections, so, let us list below only the most remarkable ones:

- The total project cost was reduced by ~21.2% and ~25.73% by considering flexible demand and vehicle-to-home capabilities, respectively. Nevertheless, the highest monetary savings were achieved when both strategies are jointly adopted, reducing the total project cost up to ~41.5%.
- The vehicle-to-home capability of the electric vehicle has a much more significant impact on the total project cost when a storage system is not installed. It has been shown that the electric vehicle may effectively play the role of a storage facility. This result is especially relevant since the exploitation of the vehicle-to-home capability may avoid the necessity of installing a battery bank.
- By considering flexibility on demand, backup generation sizing can be notably reduced. However, it has been observed that this unit is operated during more hours. This fact should be taken into account since by adopting the strategies B and D the diesel-based unit could experience a faster ageing.

The reported results demonstrate that demand-side management strategies and possible capabilities of electric vehicles should not be ignored in planning stages of isolated smart homes. Numeric results have showed an important reduction of the project cost when such aspects are considered and, therefore. These premises should be assumed in real life applications. Moreover, it has been shown that the developed optimization framework allows to observe other useful indicators that may determine to some extent the viability of the electrification project.

Ongoing works are being conducted on further exploiting the developed optimization framework to other situations in which flexible demand and vehicle-to-home capabilities may play a crucial role such as large buildings or microgrids.

7. Acknowledgments

The icons used in the figures of this paper were developed by Freepik, DinosoftLabs, Flat Icons and fjstudio from www.flaticon.com.

8. References

- [1] International Energy Agency (IEA) - World Energy Outlook 2020. Available: <https://www.iea.org/reports/world-energy-outlook-2020>, 2020 (Accessed Feb. 5 2021)
- [2] H. Louie. Off-Grid Electrical Systems in Developing Countries. Springer; Gewerbestrasse, Switzerland: 2018. <https://doi.org/10.1007/978-3-319-91890-7>
- [3] J.M. Aberilla, A. Gallego-Schmid, L. Stamford, A. Azapagic. Design and environmental sustainability assessment of small-scale off-grid energy systems for remote rural communities. Appl. Energy 2020; 258: 114004. <https://doi.org/10.1016/j.apenergy.2019.114004>
- [4] T. Jamal, C. Carter, T. Schmidt, G.M. Shafiullah, M. Calais, T. Urmee. An energy flow simulation tool for incorporating short-term PV forecasting in a diesel-PV-battery off-grid power supply system. Appl. Energy 2019; 254: 113718. <https://doi.org/10.1016/j.apenergy.2019.113718>
- [5] M. Tostado-Véliz, D. Icaza-Alvarez, F. Jurado. A novel methodology for optimal sizing photovoltaic-battery systems in smart homes considering grid outages and demand response. Renew. Energy 2021; 170: 884-96. <https://doi.org/10.1016/j.renene.2021.02.006>
- [6] U.S. Selamoğulları, T.R. Willemain, D.A. Torrey. A systems approach for sizing a stand-alone residential PEMFC power system. J. Power Sources 2007; 171(2): 802-10. <https://doi.org/10.1016/j.jpowsour.2007.06.024>

- [7] A. Chel, G.N. Tiwari, A. Chandra. Simplified method of sizing and life cycle cost assessment of building integrated photovoltaic system. *Energy Build.* 2009; 41(11): 1172-80. <https://doi.org/10.1016/j.enbuild.2009.06.004>
- [8] S.-G. Chen. An efficient sizing method for a stand-alone PV system in terms of the observed block extremes. *Appl. Energy* 2012; 91(1): 375-84. <https://doi.org/10.1016/j.apenergy.2011.09.043>
- [9] E. Kaplani, S. Kaplanis. A stochastic simulation model for reliable PV system sizing providing for solar radiation fluctuations. *Appl. Energy* 2012; 97: 970-81. <https://doi.org/10.1016/j.apenergy.2011.12.016>
- [10] H.A. Kazem, T. Khatib, K. Sopian. Sizing of a standalone photovoltaic/battery system at minimum cost for remote housing electrification in Sohar, Oman. *Energy Build.* 2013; 61: 108-15. <https://doi.org/10.1016/j.enbuild.2013.02.011>
- [11] A. Ghafoor, A. Munir. Design and economics analysis of an off-grid PV system for household electrification. *Renew. Sustain. Energy Rev.* 2015; 42: 496-502. <https://doi.org/10.1016/j.rser.2014.10.012>
- [12] C.O. Okoye, O. Solyali. Optimal sizing of stand-alone photovoltaic systems in residential buildings. *Energy* 2017; 126: 573-84. <https://doi.org/10.1016/j.energy.2017.03.032>
- [13] HOMER Pro - Microgrid software for designing optimized. Available: <https://www.homerenergy.com/products/pro/index.html>, (Accessed Feb. 18 2021)
- [14] H.U.R. Habib, S. Wang, M.R. Elkadeem, M. F. Elmorshedy. Design Optimization and Model Predictive Control of a Standalone Hybrid Renewable Energy System: A Case Study on a Small Residential Load in Pakistan. *IEEE Access* 2019; 7: 117369-90. <https://doi.org/10.1109/ACCESS.2019.2936789>
- [15] S. Rehman, H.U.R. Habib, S. Wang, M.S. Bükler, L.M. Alhems, H.Z. Al Garni. Optimal Design and Model Predictive Control of Standalone HRES: A Real Case Study for Residential Demand Side Management. *IEEE Access* 2020; 8: 29767-814. <https://doi.org/10.1109/ACCESS.2020.2972302>
- [16] E.A. Al-Ammar, H.U.R. Habib, K.M. Kotb, S. Wang, W. Ko, M.F. Elmorshedy, et al. Residential Community Load Management Based on Optimal Design of Standalone HRES With Model Predictive Control. *IEEE Access* 2020; 8: 12542-72. <https://doi.org/10.1109/ACCESS.2020.2965250>
- [17] E. Quiles, C. Roldán-Blay, G. Escrivá-Escrivá, C. Roldán-Porta. *Sustainability* 2020; 12(3): 1274. <https://doi.org/10.3390/su12031274>
- [18] C. Mokhtara, B. Negrou, A. Bouferrouk, Y. Yao, N. Settou, M. Ramadan. Integrated supply-demand energy management for optimal design of off-grid hybrid renewable energy systems for residential electrification in arid climates. *Energy Convers. Manag.* 2020; 221: 113192. <https://doi.org/10.1016/j.enconman.2020.113192>
- [19] Y. Yoshida, H. Farzaneh. Optimal Design of a Stand-Alone Residential Hybrid Microgrid System for Enhancing Renewable Energy Deployment in Japan. *Energies* 2020; 13(7): 1737. <https://doi.org/10.3390/en13071737>
- [20] N.G. Paterakis, O. Erdinç, A.G. Bakirtzis, J.P.S. Catalão. Optimal Household Appliances Scheduling Under Day-Ahead Pricing and Load-Shaping Demand Response Strategies. *IEEE Trans. Ind. Inform.* 2015; 11(6): 1509-19. <https://doi.org/10.1109/TII.2015.2438534>
- [21] M. Shafie-Khah, P. Siano. A Stochastic Home Energy Management System Considering Satisfaction Cost and Response Fatigue. *IEEE Trans. Ind. Inform.* 2017; 14(2): 629-38. <https://doi.org/10.1109/TII.2017.2728803>

- [22] S.S. Williamson. Energy Management Strategies for Electric and Plug-in Hybrid Electric Vehicles. Springer; New York, NY, USA: 2013. <https://doi.org/10.1007/978-1-4614-7711-2>
- [23] C. Liu, K. T. Chau, D. Wu, S. Gao. Opportunities and Challenges of Vehicle-to-Home, Vehicle-to-Vehicle, and Vehicle-to-Grid Technologies. Proc. IEEE 2013; 101(11): 2409-27. <https://doi.org/10.1109/JPROC.2013.2271951>
- [24] J. Chen, Y. Zhang, X. Li, B. Sun, Q. Liao, Y. Tao, et al. Strategic integration of vehicle-to-home system with home distributed photovoltaic power generation in Shanghai. Appl. Energy 2020; 263: 114603. <https://doi.org/10.1016/j.apenergy.2020.114603>
- [25] H. Shin, R. Baldick. Plug-In Electric Vehicle to Home (V2H) Operation Under a Grid Outage. IEEE Trans. Smart Grid 2017; 8(4): 2032-41. <https://doi.org/10.1109/TSG.2016.2603502>
- [26] A. Shewale, A. Mokhade, N. Funde, N.D. Bokde. An Overview of Demand Response in Smart Grid and Optimization Techniques for Efficient Residential Appliance Scheduling Problem. Energies 2020; 13(16): 4266. <https://doi.org/10.3390/en13164266>
- [27] M.S. Javadi, M. Gough, M. Lotfi, A.E. Nezhad, S.F. Santos, J.P.S. Catalão. Optimal self-scheduling of home energy management system in the presence of photovoltaic power generation and batteries. Energy 2020; 210: 118568. <https://doi.org/10.1016/j.energy.2020.118568>
- [28] R.J. Hyndman, G. Athanasopoulos. Forecasting: principles and practice, 3rd edition. OTexts, Melbourne, Australia. Available: OTexts.com/fpp3 (Accessed Apr. 5, 2021)
- [29] R. Shigenobu, A. Nakadomari, Y.-Y. Hong, P. Mandal, H. Takahashi, T. Senjyu. Optimization of Voltage Unbalance Compensation by Smart Inverter. Energies 2020; 13(18): 4623. <https://doi.org/10.3390/en13184623>
- [30] M. Collotta, G. Pau. An Innovative Approach for Forecasting of Energy Requirements to Improve a Smart Home Management System Based on BLE. IEEE Trans. Green Commun. Netw. 2017; 33(12): 2988-96. <https://doi.org/10.1109/TGCN.2017.2671407>
- [31] T.S. Ustun, S.M.S. Hussain. Standardized Communication Model for Home Energy Management System. IEEE Access 2020; 8: 180067-75. <https://doi.org/10.1109/ACCESS.2020.3028108>
- [32] K. Poncelet, E. Delarue, D. Six, J. Duerinck, W. D'haeseleer. Impact of the level of temporal and operational detail in energy-system planning models. Appl. Energy 2016; 162: 631-43. <https://doi.org/10.1016/j.apenergy.2015.10.100>
- [33] E.S. Pinto, L.M. Serra, A. Lázaro. Evaluation of methods to select representative days for the optimization of polygeneration systems. Renew. Energy 2020; 151: 488-502. <https://doi.org/10.1016/j.renene.2019.11.048>
- [34] S. Negarestani, M. Fotuhi-Firuzabad, M. Rastegar, A. Rajabi-Ghahnavieh. Optimal Sizing of Storage System in a Fast Charging Station for Plug-in Hybrid Electric Vehicles. IEEE Trans. Transp. Electrification. 2016; 2(4): 443-53. <https://doi.org/10.1109/TTE.2016.2559165>
- [35] L. Alvarado-Barrios, A.R. del Nozal, J.B. Valerino, I.G. Vera, J.L. Martínez-Ramos. Stochastic unit commitment in microgrids: Influence of the load forecasting

- error and the availability of energy storage. *Renew. Energy* 2020; 146: 2060-9. <https://doi.org/10.1016/j.renene.2019.08.032>
- [36] A. Gupte, S. Ahmed, M.S. Cheon, S. Dey. Solving mixed integer bilinear problems using MILP formulations. *SIAM J. Opt.* 2013; 23(2): 721-44. <https://doi.org/10.1137/110836183>
- [37] P. Arévalo, M. Tostado-Véliz, F. Jurado. A Novel Methodology for Comprehensive Planning of Battery Storage Systems. *J. Energy Storage* 2021; 37: 102456. <https://doi.org/10.1016/j.est.2021.102456>
- [38] S. Mandal, B.K. Das, N. Hoque. Optimum sizing of a stand-alone hybrid energy system for rural electrification in Bangladesh. *J. Clean. Prod.* 2018; 200: 12-27. <https://doi.org/10.1016/j.jclepro.2018.07.257>
- [39] D. Yang. Solar radiation on inclined surfaces: Corrections and benchmarks. *Solar Energy* 2016; 136: 288-302. <https://doi.org/10.1016/j.solener.2016.06.062>
- [40] H. Wang, K. Meng, F. Luo, Z.Y. Dong, G. Verbič, Z. Xu, et al. Demand response through smart home energy management using thermal inertia. In: *Proc Australas Univ Power Eng Conf, Hobart, TAS, 2013: 1-6.* <https://doi.org/10.1109/AUPEC.2013.6725442>
- [41] Y. Xiang, H. Cai, J. Liu, X. Zhang. Techno-economic design of energy systems for airport electrification: A hydrogen-solar-storage integrated microgrid solution. *Appl. Energy* 2020; 283: 116374. <https://doi.org/10.1016/j.apenergy.2020.116374>
- [42] European Commission. Photovoltaic Geographical Information System. Available: https://re.jrc.ec.europa.eu/pvg_tools/en/tools.html, (Accessed Feb. 22, 2021).
- [43] National Renewable Energy Laboratory (NREL). Wind Integration Data Sets. Available: <https://www.nrel.gov/grid/wind-integration-data.html>, (Accessed Apr. 6, 2021).
- [44] The World Bank. Carbon Pricing Dashboard. Available: <https://carbonpricingdashboard.worldbank.org/>, (Accessed Apr. 8, 2021).